

1 A Lagrangian analysis of ice-supersaturated air over
2 the North Atlantic

E. A. Irvine,¹ B. J. Hoskins,^{1,2} K. P. Shine¹

Corresponding author: E. A. Irvine, Department of Meteorology, University of Reading, Earley Gate, Reading, RG6 6BB, UK. (e.a.irvine@reading.ac.uk)

¹Department of Meteorology, University of Reading, Reading, UK.

²Grantham Institute for Climate Change, Imperial College London, London, UK.

3 **Abstract.** Understanding the nature of air parcels that exhibit ice-supersaturation
4 is important because they are the regions of potential formation of both cir-
5 rus and aircraft contrails, which affect the radiation balance. Ice-supersaturated
6 air parcels in the upper troposphere and lower stratosphere over the north
7 Atlantic are investigated using Lagrangian trajectories. The trajectory cal-
8 culations use ERA-Interim data for three winter and three summer seasons,
9 resulting in approximately 200,000 trajectories with ice-supersaturation for
10 each season. For both summer and winter, the median duration of ice-supersaturation
11 along a trajectory is less than 6 hours and 5% of air which becomes ice-supersaturated
12 in the troposphere will remain ice-supersaturated for at least 24 hours. In
13 winter 37% are initiated in the stratosphere and 23% of these last at least
14 24 hours. Weighting the ice-supersaturation duration with the observed fre-
15 quency indicates the likely overall importance of the longer duration ice-supersaturated
16 trajectories. Ice-supersaturated air parcels typically experience a decrease
17 in moisture content while ice-supersaturated, suggesting that cirrus clouds
18 eventually form in the majority of such air. A comparison is made between
19 short-lived (less than 24 h) and long-lived (greater than 24 h) ice-supersaturated
20 air flows. For both air flows, ice-supersaturation occurs around the north-
21 ward limit of the trajectory. Short-lived ice-supersaturated air flows show no
22 significant differences in speed or direction of movement to subsaturated air
23 parcels. However, long-lived ice-supersaturated air occurs in slower moving
24 air flows, which implies that they are not associated with the fastest mov-
25 ing air through a jet stream.

1. Key points:

- 26 1. Ice-supersaturation in ERA-Interim is investigated using Lagrangian trajectories
- 27 2. The median duration of ice-supersaturation on trajectories is less than 6 hours
- 28 3. Long-lived ice-supersaturation occurs in slowly evolving synoptic flow

2. Introduction

29 The upper troposphere contains regions of ice-supersaturation (ISS), where the relative
30 humidity with respect to ice is above 100%, and the temperature is usually defined to
31 be less than 235 K to identify only regions of ice-phase and not mixed-phase. These
32 regions are interesting for two reasons. First, given sufficiently high supersaturations,
33 regions of ISS support the formation of natural cirrus clouds by homogeneous freezing.
34 Second, the occurrence of ice-supersaturated regions in the upper troposphere and lower
35 stratosphere coincides with the cruising altitude of commercial aircraft; aircraft flying
36 through these regions may form persistent contrails which may have a relatively large, if
37 uncertain, impact on climate [*Lee et al.*, 2009; *Burkhardt and Kärcher*, 2011]. A mean
38 ISS of 15% has been observed in ice-supersaturated air in the upper-troposphere [*Gierens*
39 *et al.*, 1999]; this is below the threshold for homogeneous freezing and therefore persistent
40 contrails may form in ice-supersaturated air that is free of natural cirrus cloud.

41 The global distribution of ice-supersaturated regions (ISSRs) can be derived from satel-
42 lite data, which show that globally, the maximum frequency of occurrence is in the tropics.
43 In the mid-latitudes, high frequencies of supersaturation are coincident with the storm
44 track [*Spichtinger et al.*, 2003; *Lamquin et al.*, 2012]. ISSRs have also been diagnosed
45 using meteorological analyses, and their location linked to synoptic features. Using this

46 method, ISSRs have been found to preferentially occur in high pressure regions [*Immeler*
47 *et al.*, 2008; *Gierens and Brinkop*, 2012], in association with jet stream circulations [*Irvine*
48 *et al.*, 2012] and in warm conveyor belts associated with mid-latitude cyclones [*Spichtinger*
49 *et al.*, 2005a]. Generally, ISSRs occur in air that has experienced large-scale upward and
50 often divergent motion [*Kästner et al.*, 1999; *Gierens and Brinkop*, 2012], and are thus
51 both cooler and moister than surrounding subsaturated air [*Gierens et al.*, 1999].

52 The location and duration of ISSRs is controlled by and evolves with the synoptic flow.
53 ISSRs identified from observations or synoptic charts give us an Eulerian view of ice-
54 supersaturation. However, ISSRs are dynamic features - air flowing through a synoptic
55 pattern forms part of the ISSR when it becomes saturated, and remains part of the ISSR
56 only while saturated (this perspective is discussed in *Spichtinger et al.* [2005a]; *Schumann*
57 [2012]). Therefore the timescales of an ISSR and an ice-supersaturated air parcel are
58 different, making it difficult to diagnose from a synoptic chart how long an air parcel will
59 remain ice-supersaturated, which is an important consideration if contrails form within
60 this air parcel. Contrails formed in cold ice-supersaturated air are advected with the air
61 parcel through a weather pattern and may last for many hours; contrail cirrus outbreaks
62 have been observed to persist for 12 -18 h [*Minnis et al.*, 1998; *Duda et al.*, 2004; *Haywood*
63 *et al.*, 2009].

64 The dynamic nature of ISSRs lends itself to an alternative approach for analysing these
65 regions, by using Lagrangian trajectories. This approach has previously been applied to
66 two case studies of ISS over Germany [*Spichtinger et al.*, 2005a, b], and for a cirrus cloud
67 in an ISSR [*Montoux et al.*, 2010]. Here, we extend this approach by using trajectories
68 to characterise air flows which lead to ISS in the north Atlantic region over multiple

69 seasons. We focus on understanding long-lived ice-supersaturated air flows, which may be
70 most important to understand from a radiative perspective as they can support long-lived
71 persistent contrails and also natural cirrus clouds.

72 The method for the calculation of the Lagrangian trajectories and that used to identify
73 ice-supersaturated air are presented in Section 3 together with an example for a synoptic
74 situation with strong ridging over the north Atlantic. Properties of the ice-supersaturated
75 air parcels are analysed in Section 4.1, including the duration of ISS, the spatial distri-
76 bution of ISS and the evolution of moisture along the trajectory. Differences between air
77 parcels which have long duration and short duration ISS, such as their direction and speed
78 of movement are analysed in Section 4.2, and conclusions are presented in Section 5.

3. Methodology

3.1. Description

79 Fully Lagrangian trajectories are calculated using an offline trajectory model from
80 *Methven* [1997], where the term offline means that the wind fields are obtained di-
81 rectly from model data. The input meteorological data are 6-hourly European Centre
82 for Medium-Range Weather Forecasts Interim re-analysis data (ERA-Interim; *Dee et al.*
83 [2011]) with horizontal resolution T255 and 60 vertical levels. The Lagrangian code uses
84 a 4th order Runge-Kutta integration with a 1 hour time step to calculate the trajectories.
85 The horizontal wind fields used to advect the air parcel are taken from ERA-Interim and
86 the vertical velocity is calculated using the continuity equation. Once the position of an
87 air parcel is calculated, the gridded ERA-Interim data are then interpolated to the current
88 trajectory location.

89 Trajectories are released within the north Atlantic, defined to be the area 35-75 °N,
90 0-70 °W (shown on Figure 1(a)), on a grid with 1 ° horizontal spacing and from three
91 pressure levels: 300 hPa, 250 hPa and 200 hPa. We will refer to the time the trajectories
92 are initialised as $t=0$. From this grid, trajectories are calculated forwards in time to $t+48$
93 h and backwards in time to $t-48$ h, giving a complete trajectory length of 96 h.

94 Trajectories are initialised every 12 hours during three winters (December, January and
95 February) and three summers (June, July and August). The winters (starting December
96 1994, 1995 and 2003) and summers (1994, 1998 and 2006) were chosen for their different
97 North Atlantic Oscillation [*Barnston and Livezey, 1987*] behaviour, in order to capture a
98 range of synoptic conditions over the north Atlantic. In total, the number of trajectories
99 calculated per season exceeds 4.6 million.

100 We use both relative humidity and temperature criteria to determine whether an air
101 parcel is within a region of ice-supersaturation. A criterion that the relative humidity
102 with respect to ice is above 98% is used. We take the threshold to be below 100% firstly
103 to account for subgrid variability and secondly to account for a bias from re-calculating
104 the relative humidity from its temperature and moisture fields, that is introduced by data
105 interpolations onto different grids (personal communication Paul Berrisford, ECMWF).
106 In addition, consistent with previous studies of ISS, we apply the criterion that the tem-
107 perature should be below 235 K to avoid identifying mixed-phase regions.

108 Trajectories are released from multiple pressure levels. This could lead to a double-
109 counting of trajectories which rise from one level to another while the air is ice-
110 supersaturated. Occurrences of trajectories ascending from 300 - 250 hPa or 250 - 200
111 hPa whilst ice-supersaturated were found in fewer than 0.2% of winter trajectories. We

112 therefore assume this to have a negligible effect on our results. A second possibility, aris-
113 ing from releasing trajectories every 12 hours, is double-counting of trajectories where the
114 duration of ISS along the trajectory is greater than 12 hours. To avoid double-counting
115 ISS trajectories, we consider only those trajectories which meet the criteria for ISS at the
116 initial time ($t=0$). These trajectories are referred to as ISS trajectories; trajectories which
117 do not meet this criteria are considered as subsaturated trajectories (even if the criteria
118 are met at other points along the trajectory). Applying the above criteria results in a
119 total of 249,874 ISS trajectories in the winter data, and 188,895 in the summer data.

120 In our results we have divided the ISS trajectories into tropospheric and strato-
121 spheric. Ice-supersaturation has been observed to occur in the lower stratosphere near the
122 tropopause [*Gierens et al.*, 1999]. However, the ISS in these regions is associated with low
123 temperatures and very low specific humidities compared to such regions in the troposphere
124 [*Spichtinger et al.*, 2003] and therefore the size of the radiative effect of contrails which
125 form in these regions is uncertain. In this study, a dynamic tropopause definition of 2
126 potential vorticity units (PVU) is used, which is appropriate for the range of latitudes con-
127 sidered. Using this definition, 63% of winter ISS trajectories are classed as tropospheric
128 and 37% as stratospheric. For summer, a higher proportion, 82%, of ISS trajectories are
129 tropospheric and 18% are stratospheric. The winter numbers are in good agreement with
130 data from commercial aircraft where 38% of data showing ISS were found to be in the
131 stratosphere, using an ozone mixing ratio to define the tropopause [*Gierens et al.*, 1999].
132 Because stratospheric ice-supersaturated air is often located close to the tropopause, the
133 partitioning of ISS air into tropospheric and stratospheric has some sensitivity to the
134 tropopause definition, particularly at high latitudes; using a tropopause definition of 3

135 PVU reduces the amount of ice-supersaturated air identified as stratospheric over Green-
136 land. We defined tropospheric ice-supersaturated air to be trajectories where the first
137 point of ISS is within the troposphere, (i.e. the potential vorticity at this point is less
138 than 2 PVU), and similarly for stratospheric air.

3.2. Illustrative case study

139 As an illustration of the method used, we present a case study of trajectories initialised
140 within an ISSR. The synoptic pattern at 250 hPa is shown at $t=0$ (Figure 1(a)), cor-
141 responding to 1800 UTC 19 January 2004, when the trajectories were released. At this
142 time, there is strong ridging over the eastern north Atlantic, with a large region of ISS
143 just below the tropopause around the northern edge of the ridge. The 21 trajectories dis-
144 played on Figure 1 originated at 250 hPa from within this region of ISS (and within the
145 purple box on Figure 1(a)). The trajectories can be split into two broad groups according
146 to their pressure at $t-48$ h: one starting around 350 hPa (mostly the red trajectories on
147 Figure 1) and initially moving southwards and eastwards, and one starting around 600
148 hPa (mostly the blue trajectories on Figure 1) and ascending as they move northwards
149 and eastwards. Air moving northwards would be expected to ascend along isentropic
150 surfaces; the increase in potential temperature (Figure 1(c)), accompanied by a decrease
151 in specific humidity (not shown), suggests release of latent heat from condensation into
152 cloud droplets during this ascent. The ascent around the ridge cools the air, leading to
153 an increase in relative humidity (Figure 1(b)), and the air attains ISS around the top of
154 the ridge, and remains ISS until the air is forced to descend (Figure 1(d)) as it begins to
155 move southwards and warms. The small decrease in potential temperature whilst the air
156 is supersaturated and in the upper troposphere is consistent with radiative cooling. The

157 time from the beginning to the end of the trajectories is 96 h, showing that the large-scale
158 synoptic trough-ridge pattern persisted during this time.

159 The dynamic nature of ISSRs and the air which makes up these regions is illustrated by
160 considering their respective durations. The duration of ISS of an air parcel is defined as
161 the time period during which the air parcel is continually ice-supersaturated; the precision
162 of the calculation is therefore limited by the 6-hour time resolution of the meteorological
163 data. For example, an air parcel which is ice-supersaturated at a single point, $t=0$, along
164 a trajectory could be supersaturated for less than a single hour or just under 12 h (if
165 it becomes saturated just after $t-6$ and becomes subsaturated just before $t+6$). This is
166 likely to result in an over-estimate of the duration, therefore we take the minimum possible
167 time as the duration of ice-supersaturation: ISS at a single point is given a duration of
168 less than 6 h, at two consecutive points a duration of 6 h, at three consecutive points a
169 duration of 12 h and so on. Using this definition, for this case study, the duration of ISS
170 of the individual air parcels ranges from less than 6 hours (17 trajectories) to 12 hours (1
171 trajectory), although many remain close to saturation for 18 h; this is considerably less
172 than the duration of the ice-supersaturated region associated with the ridge. This region
173 of ISS was evident during the four days, 17-21 January 2004, that the ridge itself persisted
174 for, and disappeared only when the amplitude of the ridge had substantially decreased
175 (not shown).

4. Results

4.1. Properties of ISS trajectories

176 In this section the properties of the ISS trajectories, calculated for the three winters and
177 three summers discussed in Section 3, will be presented. Three properties are examined:

178 the duration of ISS of an air parcel, the spatial distribution of ISS and the evolution of
179 key variables while the air is ice-supersaturated.

180 A contrail formed in an ISS air parcel will be advected with the flow in that air parcel
181 (we assume any vertical motion of the contrail associated with falling ice-crystals will be
182 small), and therefore the duration of ISS is an upper-bound on the lifetime of a persistent
183 contrail. The duration of ISS along a trajectory is calculated by considering the number
184 of consecutive points of ISS along the trajectory, where the first point is obtained by
185 searching back in time from $t=0$, and the end point by searching forward in time from
186 $t=0$. This definition requires both relative humidity and temperature criteria to be met.
187 Note that a contrail, once formed, requires only the condition of relative humidity to
188 persist. Removing the temperature criterion did not significantly change the calculated
189 ISS durations.

190 The time resolution of the meteorological data used in the trajectory calculations is 6
191 hourly, which is insufficient to accurately determine the period for which an air parcel is
192 ice-supersaturated. It does, however, allow some general conclusions to be drawn. Pdfs
193 of the duration of ISS air (Figure 2) are non-Gaussian and highly-skewed towards shorter
194 durations. The median duration is less than 6 hours, i.e. ice-supersaturation was only
195 observed at a single point along the trajectory (at $t=0$). This is true for air parcels in
196 both summer and winter. The shape of the pdf is in agreement with previous studies
197 of the lifetime of satellite-observed linear contrails [*Vazquez-Navarro*, 2009] and modelled
198 contrails [*Schumann*, 2012], although we note that the tail of the distribution is longer
199 here than in *Vazquez-Navarro* [2009] probably because the method detects contrails only
200 whilst linear features and not once they have spread into contrail-cirrus. Note that the

lifetime of contrails is generally smaller than that of the ice-supersaturated air parcel they form in, since as noted by *Schumann* [2012] the air parcel must become saturated and then an aircraft must fly through it to form the contrail. In addition loss processes, such as the sedimentation of ice-particles may result in the dissipation of a contrail before the subsaturation of the ambient ice-supersaturated air.

The pdfs of ISS durations have a different shape for air which becomes ice-supersaturated in the troposphere and air which becomes ice-supersaturated in the stratosphere. In winter, air which becomes ice-supersaturated in the stratosphere has a median duration of 6h compared to less than 6h for tropospheric ISS air. A greater proportion of stratospheric ISS air, 23% compared to 5% for tropospheric air, has a duration of ISS of at least 24 h. In summer the difference is reduced; 11% of stratospheric ISS air and 5% of tropospheric ISS air have an ISS duration of at least 24 h. Note that, at the altitudes studied, a higher proportion of air parcels become ISS in the stratosphere during winter (37%) compared to summer (18%), when there is generally a higher tropopause. As noted in Section 3.1, the partitioning of ISS trajectories into tropospheric and stratospheric is sensitive to the tropopause definition; however, we note that the proportion of ISS trajectories with a lifetime of at least 24 h is increased by only a few percent if a tropopause definition of 3 PVU is used instead of the 2 PVU definition used here.

A contrail formed in an airmass for which the ISS duration is t_i is likely to persist for a time of order t_i . If we consider the overall radiative effect of a contrail to be in some way proportional to the lifetime of that contrail (note that this does not have to be a linear relationship, since contrail optical thickness may vary with time), then a measure of the total radiative effect of contrails of a certain lifetime (e.g. 0-6 h) is the number of

224 contrails of a given lifetime multiplied by that lifetime. Since we know the ISS duration,
225 and the number of trajectories of a given duration, N_i (from figures 2(a) and 2(c)), we
226 can calculate $N_i t_i$ as a proxy for this. Since the units are time, we refer to this measure
227 as the total duration. As additional motivation for this statistic, if we consider that a
228 longer-lived ISS air parcel is more likely (a) to have an aircraft fly through it and (b)
229 that a contrail formed within it will evolve into contrail cirrus, then it is useful to have a
230 measure of the overall longevity of each lifetime category. The total duration is shown on
231 Figure 2 (b) and (d). The shortest (0-6 h) ISS duration, although the most frequent, does
232 not contribute as much to the total duration of ISS air as ISS trajectories which have a
233 duration of 12 hours. The importance of stratospheric ISS air is also evident; the total
234 duration of stratospheric ISS air is larger than that of tropospheric ISS air for durations
235 greater than 18 h in winter. This shows that the contribution of stratospheric ISS air may
236 be significant, were contrails to form in it because of its longer total duration, although
237 other factors such as the temperature, available moisture and natural cloud cover are also
238 important in determining the radiative effect of such contrails. However, in summer the
239 proportion of ISS air in the stratosphere is much smaller than in the troposphere due
240 to both warmer air and a higher tropopause, therefore tropospheric ISS air has a much
241 greater total duration than stratospheric ISS air. Figure 2 shows that the total duration of
242 longer-lived ISS air is significant and hence may be important in determining the contrail
243 forcing. We will therefore give particular attention to those ISS trajectories which have a
244 long duration, defined here as continuous ice-supersaturation for at least 24 h, under the
245 assumption that these may be the most important to understand.

246 The spatial distribution of the ISS start points, the location of air when it becomes ice-
247 supersaturated, is shown in Figure 3 for trajectories released on all 3 levels, for all three
248 years of data. The outline of the north Atlantic region that the trajectories were initialised
249 in is clearly visible, due to the short duration of ISS along most of the trajectories (Figure
250 2), so to first order Figure 3 shows the actual distribution of ISS in the upper troposphere
251 within this region. The distribution of ISS compares well to previous studies [*Spichtinger*
252 *et al.*, 2003; *Lamquin et al.*, 2012; *Irvine et al.*, 2012]. The distribution of ISS start points
253 in the troposphere in winter and summer is linked to the position of the jet stream,
254 which is generally further north in summer. For stratospheric ISS trajectories, there is a
255 maximum over Greenland in winter, which is largely absent in summer when the higher
256 tropopause results in a smaller proportion of ISS air in the stratosphere at the levels used
257 in this study. There is a northward shift in the position of tropospheric ISS trajectories
258 from winter to summer, which may be caused by both temperatures rising above the
259 threshold used to avoid identifying regions of mixed-phase and a northward shift in the
260 jet stream. The spatial distribution of long-lived ISS air is broadly similar to that of all
261 ISS air for tropospheric ISS air in both seasons and for stratospheric ISS air in summer.
262 Stratospheric ISS air in winter has a region of maxima in long-lived ISS air that is shifted
263 south of the maxima for all ISS air.

264 The Lagrangian trajectories can be used to analyse the evolution of the moisture content,
265 pressure and temperature of an air parcel, to determine which has a greater control on
266 the duration of ISS. Previous studies have shown that lifting and cooling of air is the
267 main pathway to ISS [*Gierens et al.*, 1999; *Spichtinger et al.*, 2005a], but it is unclear
268 whether drying or sinking and warming have the biggest effect on the duration of ISS.

269 First, we analyse the evolution of the moisture content of ice-supersaturated air. Pdfs of
270 the change in specific humidity and pressure during the period of ISS are shown in Figure
271 4, for trajectories where ISS is observed at a minimum of two consecutive points along
272 the trajectory (corresponding to a duration of at least 6 h). Specific humidity decreases
273 by up to 80% during the ISS duration (Figure 4(a)), while the air undergoes weak ascent
274 of typically less than 20 hPa (Figure 4(b)) at the same time. The decrease in specific
275 humidity during the period of ISS is consistent with condensation processes from cloud
276 formation, which suggests that cirrus cloud eventually forms in the majority of air masses
277 that become ice-supersaturated, although we lack the relevant model data to confirm
278 this. This would agree with lidar observations of ice-supersaturated regions which show
279 the majority of ice-supersaturated air also contains ice particles [Immler *et al.*, 2008], so
280 that contrails are often observed embedded in thin or subvisible cirrus [Immler *et al.*,
281 2008; Voigt *et al.*, 2010; Iwabuchi *et al.*, 2012]. To assess the importance of these moisture
282 changes on the duration of ISS, we re-calculated the relative humidity at the first point
283 of subsaturation after the period of ISS, using (1) the specific humidity from the first
284 point of ISS, (2) the specific humidity from the last point of ISS and (3) the pressure and
285 temperature from the last point of ISS, for winter trajectories released from 250 hPa. For
286 scenario (1) the air parcel is now ISS in 76% of trajectories, showing that the total loss
287 of water over time does contribute to limiting the duration of ISS. For scenario (3) 60%
288 of trajectories are now ISS whereas for scenario (2) only 30% of trajectories are ISS. This
289 shows that drying and sinking of air parcels are the major controls on the duration of ISS
290 of an air parcel, but the cumulative loss of moisture over time is a contributing factor.

4.2. A comparison of short and long duration ISS air

291 In this section the recent history of air parcels is considered to determine differences
292 between airflows which lead to ice-supersaturation and those which do not. Differences
293 between the recent history of long-duration (at least 24 h) ISS air and shorter-duration
294 (less than 24 h) ISS air are also investigated to understand whether it might be possible
295 to know a priori whether an air parcel will remain in an ice-supersaturated state for
296 a significant period of time. This is important to understand from the perspective of
297 the formation of long-lived contrails in such air parcels and their possible evolution into
298 contrail cirrus.

299 The 24 h period leading up to ISS (or the 24 h period prior to $t=0$ for subsaturated air)
300 is used to investigate the recent history of supersaturated and subsaturated air masses.
301 Three variables are analysed: the speed of air and the change in pressure along a trajectory,
302 and the direction of movement. The speed of air along a trajectory is the wind speed in the
303 region of the trajectory, since the trajectories are calculated by using the horizontal wind
304 components to advect air parcels. Equally, the change in pressure along the trajectories
305 is the vertical motion of the ambient air, with negative values implying ascent. Pdfs of
306 wind speed and vertical motion are shown in Figure 5, for both ISS air and subsaturated
307 air, which is used as a climatology. In winter (Figure 5(a)), the speed of subsaturated
308 air has a Gaussian distribution, with a peak around 30 m s^{-1} and a tail out to 70 m
309 s^{-1} indicative of air flowing through the jet stream. The pdf for shorter-lived ISS air
310 is almost identical to subsaturated air. In contrast, for long-lived ISS the distribution is
311 highly skewed towards smaller speeds with a peak at around 10 m s^{-1} . In summer (Figure
312 5(c)), the distribution of the speed of subsaturated air peaks at lower speeds of around
313 20 m s^{-1} and the tail cuts-off at smaller speeds than in winter. As for winter, long-lived

314 ISS air is associated with smaller wind speeds than shorter-lived ISS air, although the
315 difference is less-pronounced, due to the smaller range of wind speeds observed at these
316 altitudes in summer when the jet stream is weaker.

317 The distribution of the change in pressure along a trajectory peaks around zero for
318 subsaturated air, and contains both ascent and descent. In contrast, whilst pdfs for
319 both long and short-lived ISS air have a peak near zero ascent, they contain almost
320 no values of descent; as expected, both shorter-lived and long-lived ISS occurs in air
321 which has ascended. This is consistent with the assumption from *Gierens and Brinkop*
322 [2012] that the descent they found in pdfs of vertical velocity of ISSRs is associated with
323 decaying ISSRs. In winter, the distribution of pressure change for long-lived ISS air
324 has a peak at smaller values of ascent and a smaller variance compared to shorter-lived
325 ISS air (Figure 5(b)). In summer, the peak of both distributions are similar (Figure
326 5(d)), with larger frequencies of strong ascent for the shorter-lived ISS air. Considering
327 the distributions of speed and pressure change together, the slower wind speeds and
328 smaller ascent of long-lived ISS air suggest that it occurs in more slowly evolving weather
329 situations. The rate of change of temperature, pressure and specific humidity during the
330 period of ice-supersaturation is slower in longer-lived ISS trajectories (not shown), which
331 further supports this hypothesis.

332 Similarly, we can construct pdfs of the direction that the air moved in the 24 h leading
333 up to the first point of ISS, and the 24 h following the first point of ISS, for subsaturated
334 air (the climatology), shorter-lived and long-lived ISS air. Here, the results are split
335 by region, to allow for the different synoptic regimes which might influence the flow in
336 each region. Four sub-regions of interest are defined, based on the spatial distribution of

337 the ISS start points in Figure 3. We refer to these as: Atlantic-European, Mid-Atlantic,
338 Greenland and Iceland; their locations are shown as boxes on Figure 6(a). For each region,
339 we consider only those tropospheric ISS trajectories where the first point of ISS is within
340 the region of interest. Winter data is shown for all regions except Iceland, which has a
341 larger number of ISS points in summer.

342 An example of the movement of air along ISS trajectories is shown in Figure 6 for long-
343 lived tropospheric ISS air which becomes ice-supersaturated within the Atlantic-European
344 and mid-Atlantic regions. The location of these trajectories 24 h prior to becoming ice-
345 supersaturated within these regions, and their subsequent location 24 h later, gives an
346 indication of the synoptic conditions in which the ISS occurred. Air which becomes ice-
347 supersaturated over the Atlantic-European region comes predominantly from the west and
348 south-west (Figure 6(a)). However, air which becomes ice-supersaturated over the mid-
349 Atlantic region comes from a westerly direction (Figure 6(c)), and in general has moved
350 further than air which becomes ice-supersaturated over the Atlantic-European region,
351 suggesting the influence of the jet stream. 24 h after air becomes ice-supersaturated in
352 either region, when it is still supersaturated, it has moved towards the north and east.
353 In the case of persistent contrail formation within these air parcels, contrails which are
354 formed over the region of interest would be advected towards the north and east, to the
355 regions shown in Figure 6(b, d). This information can be summarised as pdfs to show the
356 movement of air leading up to and following ISS, for the different regions (Figures 7 and
357 8).

358 Pdfs of the direction of movement leading up to ISS are shown in Figure 7. For all
359 regions, the distributions for shorter-lived ISS air are similar to those for subsaturated

360 air, i.e. are similar to climatology. For the Atlantic-European region (Figure 7(a)) and
361 mid-Atlantic region (Figure 7(b)) in winter, which are dominated by the jet stream, flow
362 is predominantly from the west. However, the distribution for longer-lived ISS air shows
363 a higher proportion of southerly winds than subsaturated or shorter-lived ISS air. This
364 is also true for the Iceland region in summer (Figure 7(d)), where longer-lived ISS air
365 has a higher proportion of flow from the south-west than shorter-lived ISS air. For the
366 Greenland region in winter (Figure 7(c)), the distribution is broader, meaning that the
367 direction of flow is more variable. This region is generally north of the influence of the
368 jet stream and can have weak upper-level flow. For both Greenland and Iceland regions,
369 a greater proportion of the flow comes from an easterly direction.

370 Further information about the airflows leading to ISS is obtained by considering the
371 direction of flow during the 24 h following the first point of ISS. This is shown for all regions
372 in Figure 8. Once again the pdfs of direction of movement are similar for subsaturated air
373 and shorter-lived ISS air, indicating that using this method we cannot use flow direction
374 alone to distinguish between subsaturated and short-lived ISS air. For the Atlantic-
375 European and mid-Atlantic regions (Figures 8(a) and 8(b)), for subsaturated and short-
376 lived ISS air, the bulk of the pdf has shifted from flow from the south-west quadrant to
377 flow from the north-west quadrant. However, for long-lived ISS air the peak is from the
378 south-west, indicating that these airflows are still moving north (consistent with Figure
379 6(b)) and therefore likely to be experiencing ascent. If, we consider instead the direction
380 of flow in the 24 h following the last point of ISS (not shown), we find that the long-lived
381 ISS air now has a northerly component, consistent with the air descending and becoming
382 subsaturated. The difference between short and long-lived ISS airflows is less clear for

383 the Greenland and Iceland regions, as the variance of the pdfs is large indicating that the
384 flow direction is very variable in these regions.

385 Put together, these results suggest that ice-supersaturation occurs around the northward
386 limit of the trajectory. This suggests that long-lived ISS air primarily occurs in two
387 different synoptic situations: slower-moving air ascending around the periphery of an
388 anticyclone, and air rising in the jet stream circulations (regions of ascent in the right jet
389 entrance and left jet exit), that are on the edge of the circulation rather than in the core
390 of the jet.

5. Conclusions

391 Ice-supersaturated air parcels have been analysed using Lagrangian trajectories. These
392 highlight the dynamical nature of ice-supersaturated regions that can be readily diagnosed
393 from observational data and meteorological analyses; here we investigate the air which
394 makes up these regions. Trajectories have been calculated from ERA-Interim data for
395 three winter and three summer seasons, giving a large data sample of trajectories which
396 contain ice-supersaturation.

397 The duration of ice-supersaturation is generally short-lived; the median duration of ISS
398 is less than 6 h for both winter and summer seasons. In winter, the median duration of
399 stratospheric ISS air is longer at 6 h, although this could be an artefact of the coarse
400 time resolution of the meteorological data. 5% of tropospheric ISS trajectories have a
401 duration of at least 24 h. In winter, a large proportion of trajectories, 37%, become ISS
402 in the stratosphere, and of these 23% have an ISS duration of at least 24 h. We note
403 that, whilst the partitioning of ISS trajectories into tropospheric and stratospheric has
404 some sensitivity to the tropopause definition, the effect on the distributions of the ISS

405 duration is small. The percentage of ISS air which remains in a supersaturated state for
406 at least 24 h is higher than previous studies of contrail lifetimes (e.g. *Schumann* [2012]).
407 This is expected, since the duration of ISS air is an upper-bound on the lifetime of a
408 contrail forming in that air mass, and loss processes such as sedimentation of ice crystals
409 are not accounted for here. Weighting the ice-supersaturation duration with the observed
410 frequency indicates the likely overall importance of the longer duration ice-supersaturated
411 trajectories, which are a focus of this study.

412 The evolution of the properties of the air parcel whilst it is supersaturated show that air
413 parcels continue to ascend whilst saturated, and lose moisture. The decrease in moisture
414 content could be explained by the formation of cirrus clouds in the ISS air. In this study
415 we have not considered the presence of natural cirrus clouds in the ice-supersaturated
416 air. To do so would require interpolating cloud cover fraction to the location of the
417 trajectories, which could introduce spurious results since cloud cover is not a continuous
418 field. Whilst our results seem to suggest that natural cirrus cloud would eventually form
419 in the majority of air parcels which remain supersaturated for a long period of time,
420 further studies would be required to confirm this. The total loss of moisture while the air
421 parcel is supersaturated does play a role in limiting the duration of ISS, however a major
422 control on the ISS duration is descent and warming of the air parcel.

423 We have analysed the history of air masses to discern differences between subsaturated
424 air and ISS air of short and long duration. For both long and short-lived ISS, the airflow
425 leading to ice-supersaturation is predominantly westerly. However this turns from having
426 a southerly to northerly component after (the last point of) saturation, and only weak
427 ascent. This suggests that the ISS occurs around the northward limit of the trajectory.

428 In general, long-lived trajectories exhibit different behaviour to shorter-lived trajectories;
429 they occur in slower moving air which is ascending more slowly which implies they are
430 not associated with fast (or the fastest) moving air through a jet stream. The direction of
431 air leading up to ISS also shows a higher proportion of southerly winds than climatology,
432 and the air continues to have a northward component and rise whilst saturated. However,
433 considering the recent history (the previous 24 h) of short-duration ISS air and subsatu-
434 rated air the only difference is that subsaturated air may experience descent in its recent
435 history, whereas short-lived ISS air does not.

436 Lagrangian trajectories provide a dynamical perspective on ice-supersaturated air, and
437 have previously only been used in a case study approach. Here we have extended their
438 use to calculate trajectories for extended periods, to obtain a large sample of trajectories
439 containing ice-supersaturation. The trajectories are useful as an upper-bound of the
440 duration of potential contrails forming within ice-supersaturated air parcels, however they
441 are subject to the limits of the models capability to represent ice-supersaturation. In this
442 study we have not tried to separate out ISS trajectories into different weather situations,
443 to explain the variety of contrail durations. The results of this study suggest that at
444 least long-lived ISS occurs preferentially in some airflows but fails to discern differences
445 between short-lived ISS and subsaturated airflows, beyond confirming that ISS air occurs
446 in rising airflows. These results contribute to a better understanding of the dynamical
447 nature of ice-supersaturated regions which is important for evaluating predictions of ice-
448 supersaturation from numerical weather prediction or climate models.

449 **Acknowledgments.** This work is part of the REACT4C project, funded under the
450 EU 7th framework programme, grant ACP8-GA-2009-233772. The Lagrangian trajectory

code was provided by John Methven. We thank Klaus Gierens for comments on an earlier
draft of the paper.

References

- Barnston, A. G., and R. E. Livezey (1987), Classification, seasonality and persistence of
low-frequency atmospheric circulation patterns, *Mon. Wea. Rev.*, *115*, 1083–1126.
- Burkhardt, U., and B. Kärcher (2011), Global radiative forcing from contrail cirrus, *Nature
Climate Change*, *1*, 54–58, doi:10.1038/nclimate1068.
- Dee, D. P., et al (2011), The ERA-Interim reanalysis: configuration and performance of
the data assimilation system, *Q. J. R. Meteorol. Soc.*, *137*, 553–597, doi: 10.1002/qj.828.
- Duda, D. P., P. Minnis, L. Nguyen, and R. Palikonda (2004), A case study of the de-
velopment of contrail clusters over the Great Lakes, *J. Atmos. Sci.*, *61*, 1132–1146,
doi:10.1175/1520-0469(2004)061.
- Gierens, K., and S. Brinkop (2012), Dynamical characteristics of ice-supersaturated re-
gions, *Atmos. Chem. Phys.*, *12*, 11,933–11,942, doi:10.5194/acp-12-11933-2012.
- Gierens, K. M., U. Schumann, H. G. J. Smit, M. Helten, and A. Marenco (1999), A
distribution law for relative humidity in the upper troposphere and lower stratosphere
derived from three years of MOZAIC measurements, *Ann. Geophysicae*, *17*, 1218–1226,
doi:10.1007/s00585-999-1218-7.
- Haywood, J. M., R. P. Allan, J. Bornemann, P. M. Forster, P. N. Francis, S. Milton,
G. Rädcl, A. Rap, K. P. Shine, and R. Thorpe (2009), A case study of the radiative
forcing of persistent contrails evolving into contrail-induced cirrus, *J. Geophys. Res.*,
114, D24,201, doi:10.1029/2009JD012650.

- 472 Immler, F., R. Treffeisen, D. Engelbart, K. Krüger, and O. Schrems (2008), Cirrus, con-
473 trails, and ice supersaturated regions in high pressure systems at northern mid-latitudes,
474 *Atmos. Chem. Phys.*, *8*, 1689–1699, doi:10.5194/acp-8-1689-2008.
- 475 Irvine, E. A., B. J. Hoskins, and K. P. Shine (2012), The dependence of contrail formation
476 on the weather pattern and altitude in the North Atlantic, *Geophys. Res. Lett.*, *39*,
477 L12,802, doi:10.1029/2012GL051909.
- 478 Iwabuchi, H., P. Yang, K. N. Liou, and P. Minnis (2012), Physical and optical properties
479 of persistent contrails: climatology and interpretation, *J. Geophys. Res.*, *117*, D06,215,
480 doi:10.1029/2011JD017020.
- 481 Kästner, M., R. Meyer, and P. Wendling (1999), Influence of weather conditions on the
482 distribution of persistent contrails, *Meteorol. Appl.*, *6*, 261–271.
- 483 Lamquin, N., C. J. Stubenrauch, K. Gierens, U. Burkhardt, and H. Smit (2012), A global
484 climatology of upper-tropospheric ice supersaturation occurrence inferred from the At-
485 mospheric Infrared Sounder calibrated by MOZAIC, *Atmos. Chem. Phys.*, *12*, 381–405,
486 doi:10.5194/acp-12-381-2012.
- 487 Lee, D. S., D. W. Fahey, P. M. Forster, P. J. Newton, R. C. N. Wit, L. L. Lim, B. Owen,
488 and R. Sausen (2009), Aviation and global climate change in the 21st century, *Atmo-
489 spheric Environment*, *43*, 3520–3537, doi:10.1016/j.atmosenv.2009.04.024.
- 490 Methven, J. (1997), Offline trajectories: calculation and accuracy, *Tech. Report 44*, U. K.
491 *Univ. Global Atmos. Modelling Programme*, 18pp.
- 492 Minnis, P., D. F. Young, D. P. Garber, L. Nguyen, W. L. Smith Jr., and R. Palikonda
493 (1998), Transformation of contrails into cirrus during SUCCESS, *Geophys. Res. Lett.*,
494 *25*, 1157–1160, doi: 10.1029/97GL03314.

- 495 Montoux, N., P. Keckhut, A. Hauchecorne, J. Jumelet, H. Brogniez, and C. David
496 (2010), Isentropic modelling of a cirrus cloud event observed in the midlati-
497 tude upper troposphere and lower stratosphere, *J. Geophys. Res.*, *115*, D02,202,
498 doi:10.1029/2009JD011981.
- 499 Schumann, U. (2012), A contrail cirrus prediction model, *Geosci. Model Dev.*, *5*, 543–580,
500 doi: 10.5194/gmd-5-543-2012.
- 501 Spichtinger, P., K. Gierens, and W. Read (2003), The global distribution of ice-
502 supersaturated regions as seen by the microwave limb sounder, *Q. J. R. Meteorol. Soc.*,
503 *129*, 3391–3410, doi: 10.1256/qj.02.141.
- 504 Spichtinger, P., K. Gierens, and H. Wernli (2005a), A case study on the formation and
505 evolution of ice supersaturation in the vicinity of a warm conveyor belt’s outflow region,
506 *Atmos. Chem. Phys.*, *5*, 973–987, doi:10.5194/acp-5-973-2005.
- 507 Spichtinger, P., K. Gierens, and A. Dörnbrack (2005b), Formation of ice supersaturation
508 by mesoscale gravity waves, *Atmos. Chem. Phys.*, *5*, 1243–1255, doi:10.5194/acp-5-1243-
509 2005.
- 510 Vazquez-Navarro, M. R. (2009), Life cycle of contrails from a time series of geostationary
511 satellite images, *PhD Thesis, Deutsches Zentrum für Luft und Raumfahrt*.
- 512 Voigt, C., et al. (2010), In-situ observations of young contrails - overview and selected re-
513 sults from the concert campaign, *Atmos. Chem. Phys.*, *10*, 9039–9056, doi: 10.5194/acp-
514 10-9039-2010.

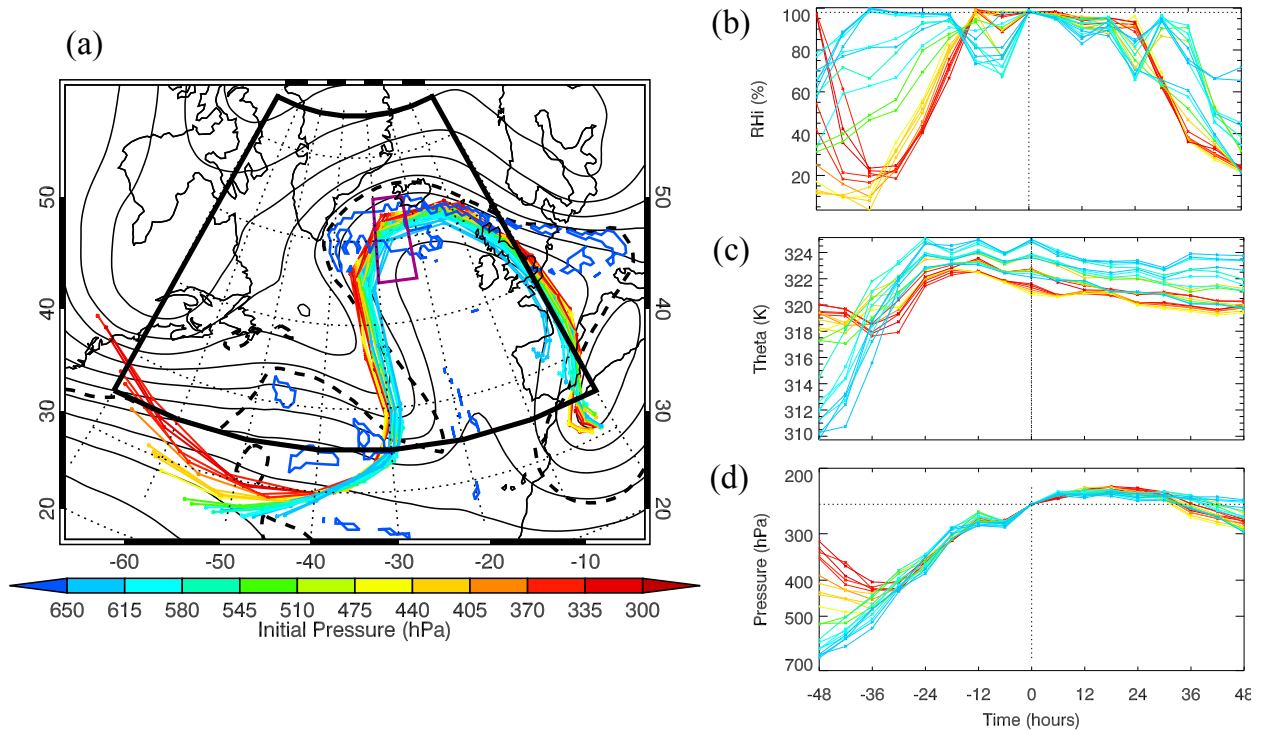


Figure 1. (a) An example of trajectories initialised within the purple box at 250 hPa; only trajectories which were within the ice-supersaturated region (blue contours) are shown. The trajectories are released at $t=0$, corresponding to 1800 UTC 19 January 2004. The synoptic pattern at this time is shown by the 250 hPa geopotential height (thin black contours), the dynamical tropopause is displayed using the PV2 contour (thick dashed black line) and regions of ice-supersaturation at 250 hPa are outlined in blue. The path of the ISS trajectories is shown from $t-48$ to $t+48$, coloured by the pressure of the air at $t-48$. The black box defines the north Atlantic region that the trajectories used in this study were initialised in. For the same period, (b) the relative humidity calculated with respect to ice, (c) potential temperature (theta) and (d) pressure along the trajectories.

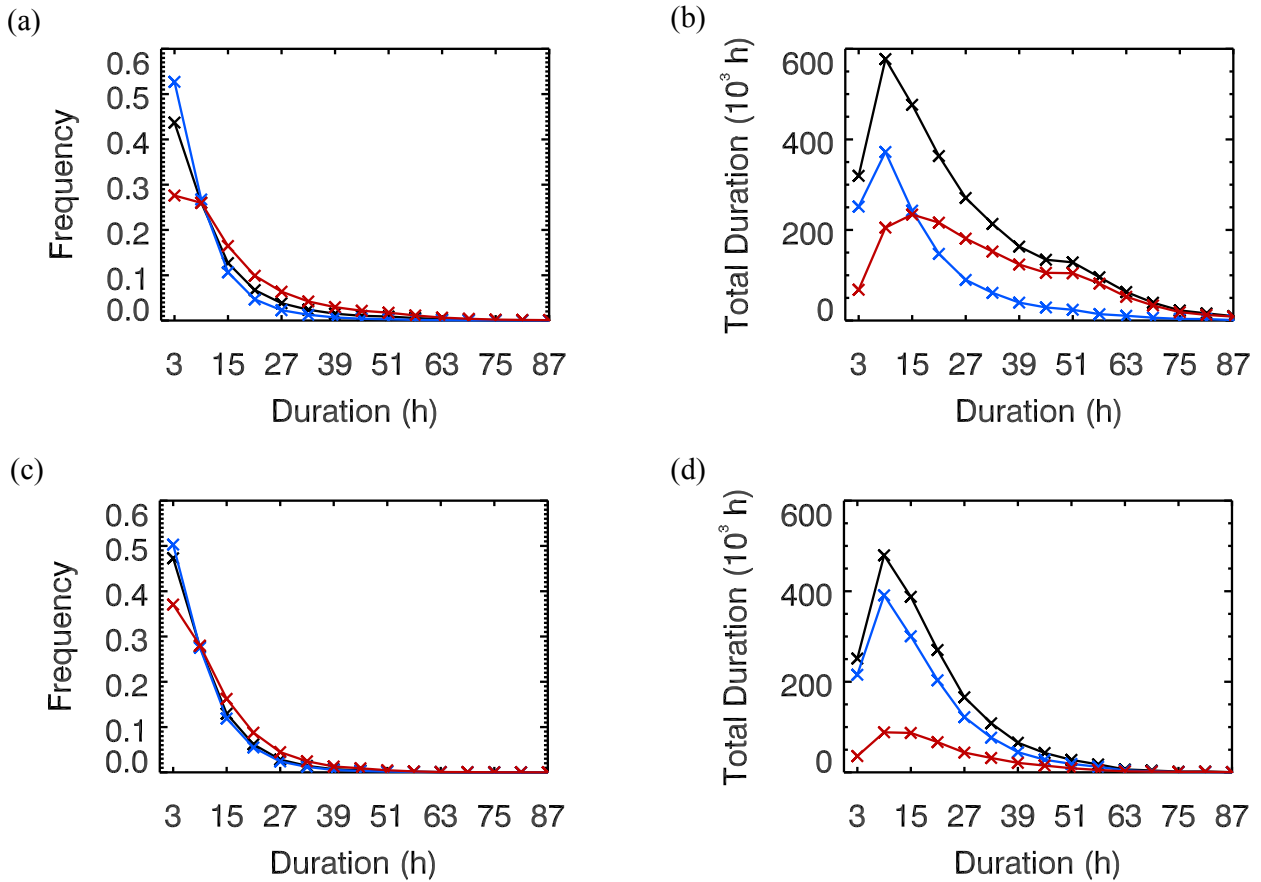


Figure 2. Histograms of the duration of ice-supersaturation calculated along air parcel trajectories, for trajectories released from all three pressure levels for (a) all three winters and (c) all three summers, using duration bins of 6 h. The three lines correspond to all ISS trajectories (black), tropospheric ISS air (blue) and stratospheric ISS air (red). Histograms of the total duration in units of 10^3 h, calculated for each duration bin as the median duration multiplied by the number of trajectories with that duration, (b) for winter and (d) for summer.

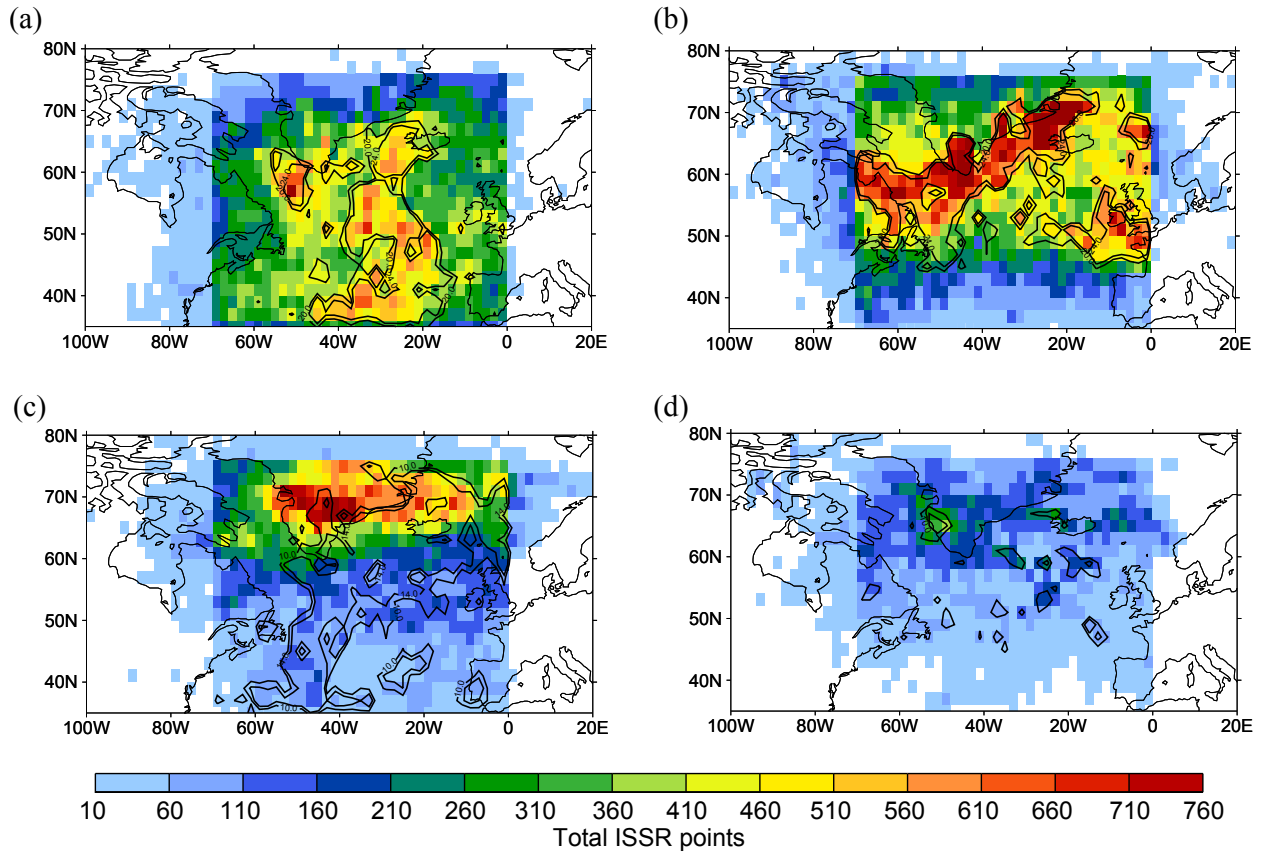


Figure 3. Map of the density of points where air first becomes ISS along a trajectory for all trajectories (colours) and long-lived ISS air (black contours) for (a) tropospheric winter, (b) tropospheric summer, (c) stratospheric winter and (d) stratospheric summer trajectories. Data have been gridded into 2° boxes before plotting. Note the difference in the line contour scale for long-lived ISS air between the top and bottom panels: the minimum contour level in (a), (b) is 20 and in (c), (d) is 10 trajectories.

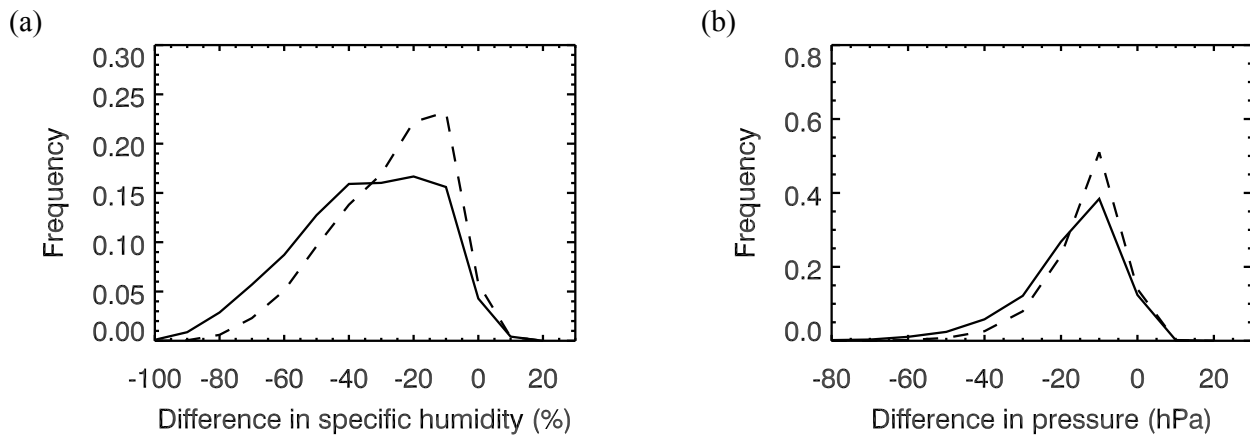


Figure 4. Change in (a) specific humidity and (b) pressure between the last point of ISS and first point of ISS along ISS trajectories released from 250 hPa in winter (solid line) and summer (dashed line). Negative changes in specific humidity indicate drying and negative changes in pressure indicate ascent during the period of ISS.

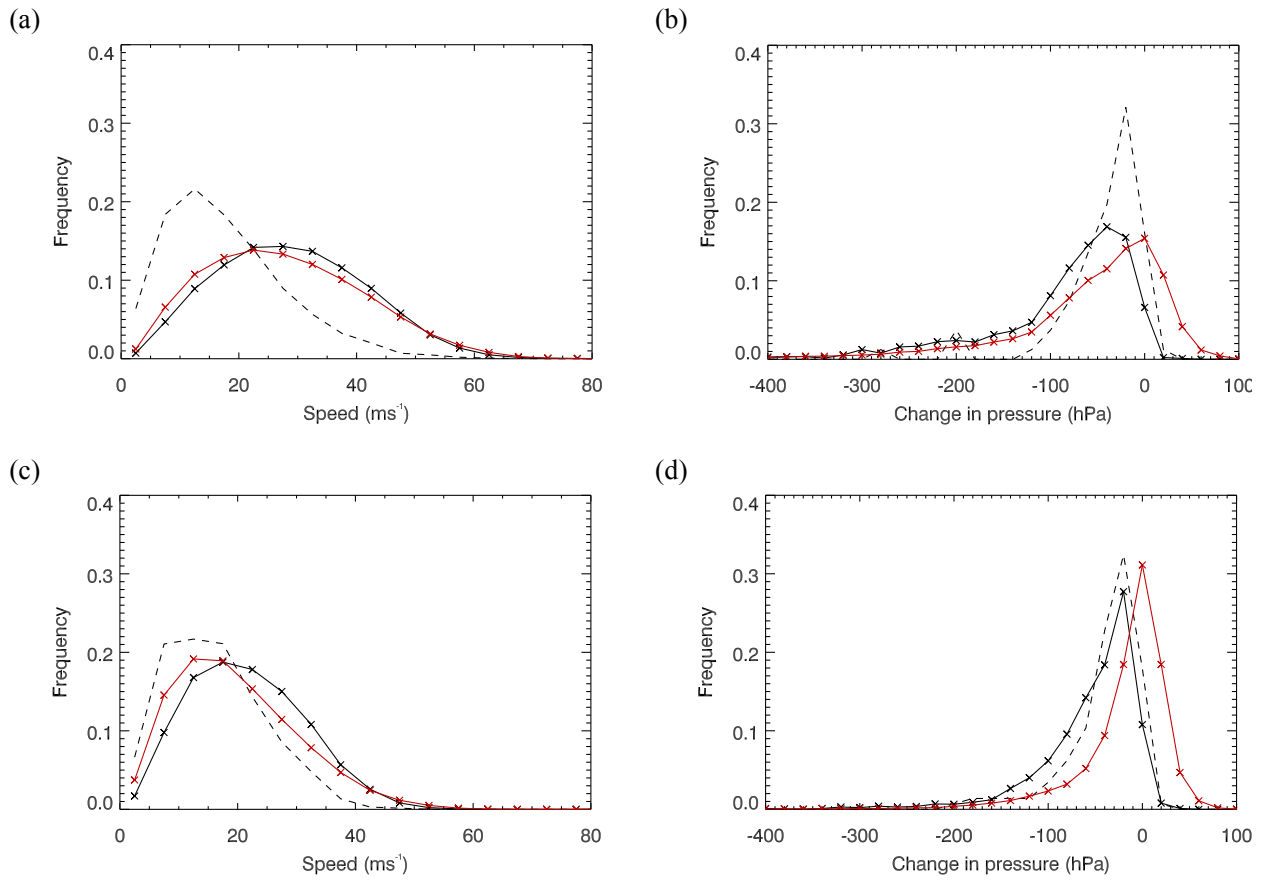


Figure 5. For the 24 h period prior to air becoming ISS, (a) the speed of air and (b) the change in pressure along the trajectory, for winter trajectories released from all three levels. (c), (d) as for (a), (b) but for summer trajectories. Change in pressure calculated as the pressure at the time the air parcel becomes supersaturated minus the pressure 24 hrs prior to this. Negative values imply parcel ascent. Shown for: tropospheric ISS air with a lifetime less than 24 h (black solid line), tropospheric ISS air with a lifetime of at least 24 h (black dashed line) and subsaturated air (red line).

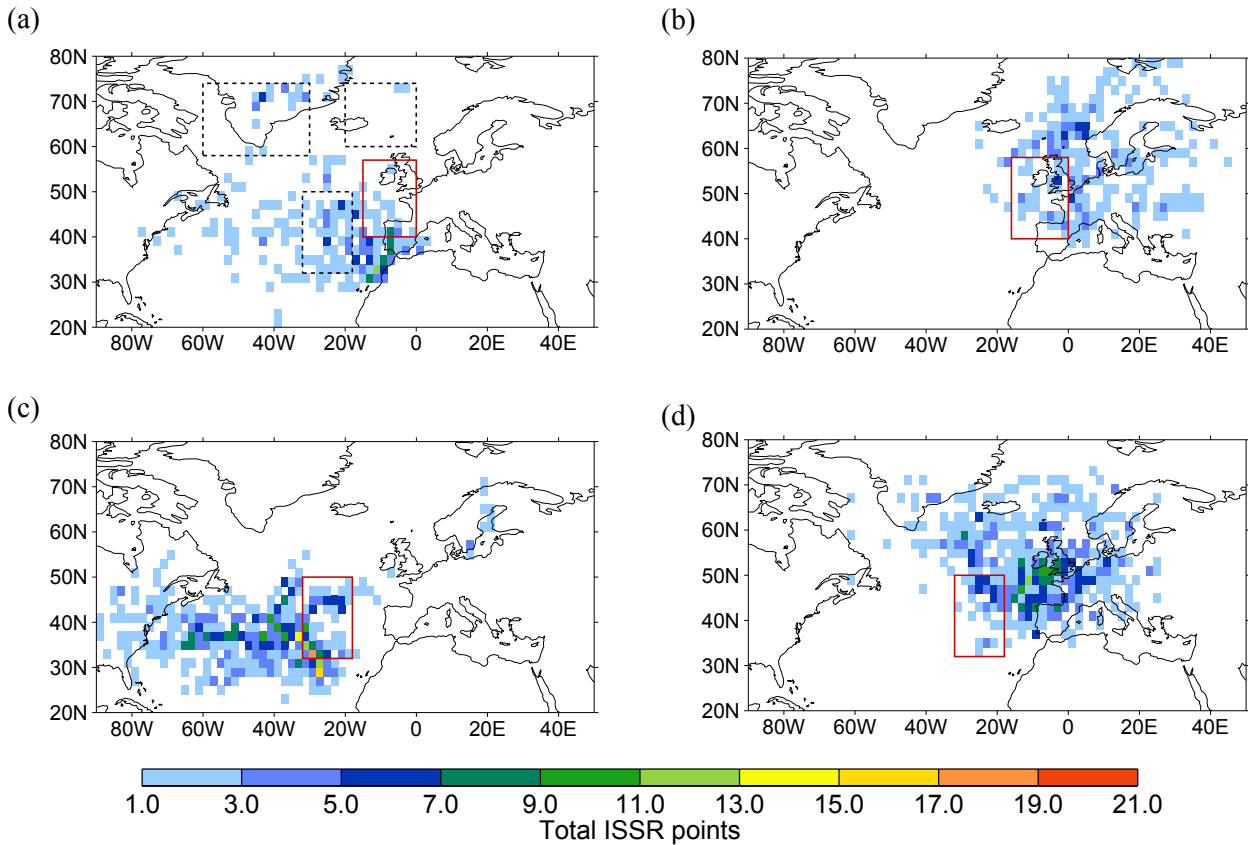


Figure 6. For ISS trajectories released from all levels in winter, whose the first point of ISS is within the Atlantic-European region (defined by the red box, top row) or mid-Atlantic region (bottom row), a density map of the location of this air (a, c) 24 h prior to, and (b, d) 24 h subsequent to this time. For tropospheric ISS air with an ISS lifetime of at least 24 h. The locations of all regions are marked as boxes on (a).

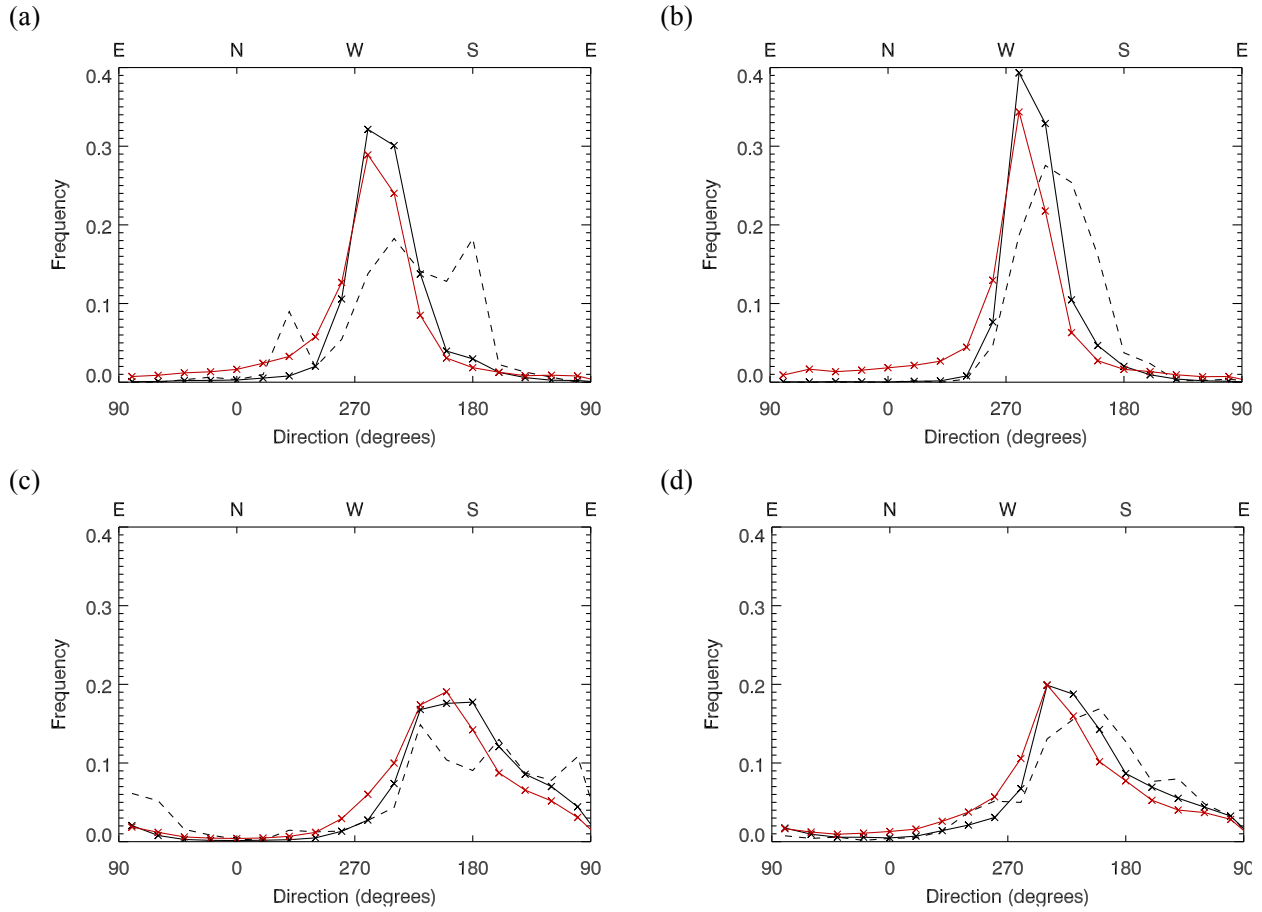


Figure 7. The direction of movement of air along a trajectory in the 24 h leading up to ISS, for regions (a) Atlantic-Europe in winter, (b) mid-Atlantic in winter, (c) Greenland in winter and (d) Iceland in summer, for trajectories released from all three levels. Shown for: tropospheric ISS air with a lifetime less than 24 h (black solid line), tropospheric ISS air with a lifetime of at least 24 h (black dashed line) and subsaturated air (red line).

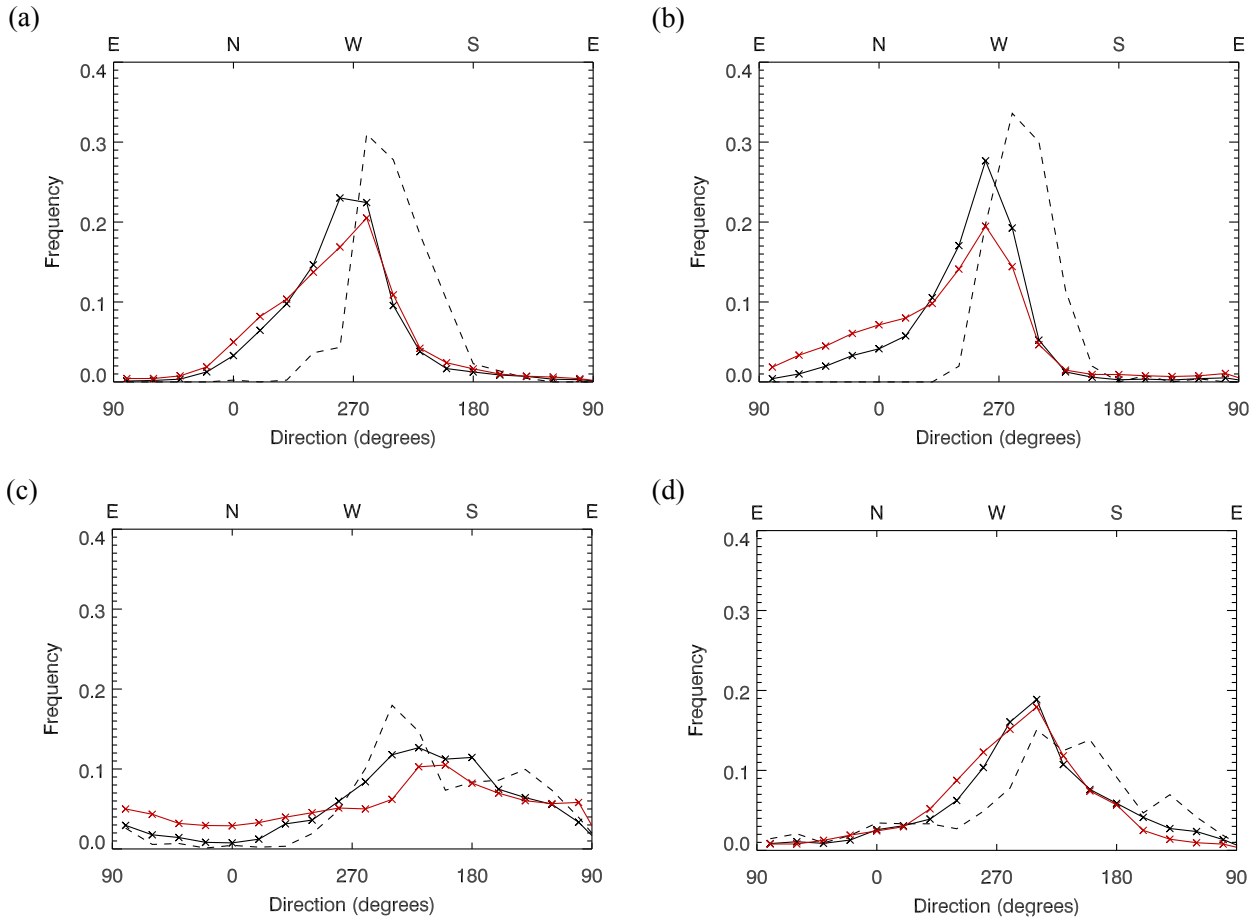


Figure 8. The direction of movement of air along a trajectory in the 24 h following the first point of ISS, for regions (a) Atlantic-Europe in winter, (b) mid-Atlantic in winter, (c) Greenland in winter and (d) Iceland in summer, for trajectories released from all three levels. Shown for: tropospheric ISS air with a lifetime less than 24 h (black solid line), tropospheric ISS air with a lifetime of at least 24 h (black dashed line) and subsaturated air (red line).